J. Biochem. 2011;150(1):103–111 doi:10.1093/jb/mvr040

JB THE JOURNAL OF BIOCHEMISTRY

Genetic interactions of ribosome maturation factors Yvh1 and Mrt4 influence mRNA decay, glycogen accumulation, and the expression of early meiotic genes in *Saccharomyces cerevisiae*

Received February 28, 2011; accepted March 9, 2011; published online April 6, 2011

Minetaka Sugiyama, Satya Nugroho*, Naoko Iida†, Taiki Sakai‡, Yoshinobu Kaneko and Satoshi Harashima§

Department of Biotechnology, Graduate School of Engineering, Osaka University, 2-1 Yamadaoka, Suita, Osaka 565-0871, Japan

*Present address: Satya Nugroho, Research Centre for Biotechnology, LIPI, Jl. Raya Bogor Km 46, Cibinong 16 911, Indonesia.
†Present address: Naoko Iida, Laboratory of Mutagenesis, National Institute of Genetics, Japan, Yata 1111, Mishima, Shizuoka 411-8540, Japan.
‡Present address: Taiki Sakai, Tatsuuma-Honke Brewing Company Limited, 2-10, Tateishi, Nishinomiya, Hyogo 662-8510, Japan.
§Satoshi Harashima. 2-1 Yamadaoka, Suita, Osaka 565-0871, Japan. Tel: +81-(0)6-6879-7420, Fax: +81-(0)6-6879-7421, email: harashima@bio.eng.osaka-u.ac.jp

The *Saccharomyces cerevisiae* Yvh1, a dual-specificity protein phosphatase involved in glycogen accumulation and sporulation, is required for normal vegetative growth. To further elucidate the role of Yvh1, we generated dominant mutants suppressing the slow growth caused by *YVH1* disruption. One of the mutant alleles, designated as *SVH1-1* (suppressor of *yvh1* deletion), was identical to *MRT4* (mRNA turnover) that contained a single-base substitution causing an amino acid change from Gly[68] to Asp. Mrt4(G68D) restored the deficiencies in growth and rRNA biogenesis that occurs in absence of Yvh1. Here, we report that the interaction between Mrt4 and Yvh1 is also essential for normal glycogen accumulation and mRNA decay as well as the induction of sporulation genes *IME2*, *SPO13* and *HOP1*. The Mrt4(G68D) could restore the plethora of phenotypes we observed in absence of Yvh1. We found that Yvh1 is not essential for wild-type induction of the transcriptional regulator of these genes, *IME1*, suggesting that either translation or post-translational modification to activate Ime1 has been compromised. Since a defect in ribosome biogenesis in general can be related to other various defects, the ribosome biogenesis defect caused by absence of Yvh1 might be an indirect cause of observed phenotypes.

Keywords: glycogen/Mrt4/*Saccharomyces cerevisiae*/sporulation/Yvh1.

Abbreviations: CgTRP1, Candida glabrata TRP1; CgHIS3, Candida glabrata HIS3; ETS, external transcribed spacer; ITS, internal transcribed spacer; *S. cerevisiae*, *Saccharomyces cerevisiae*.

Protein phosphorylation and dephosphorylation are central to many mechanisms that regulate cellular activities in both prokaryotic and eukaryotic organisms (*1*). During signal transduction, for example, a cascade of factors interacts depending on their phosphorylation status, resulting in the regulation of gene expression. In an organism, there are generally more protein kinases, which are responsible for protein phosphorylation, than phosphatases, which mediate protein dephosphorylation, although both protein super-families are equally important for cellular processes.

In the genome of *Saccharomyces cerevisiae* genes, for 117 protein kinases and 37 protein phosphatases have been identified (http://proteome.com). Since, we began our project to elucidate the functions of 30 non-essential *S. cerevisiae* protein phosphatases, we have disrupted each of their genes and created for all possible combinations double-disruption mutants, followed by phenotypic analysis (*2*, *3*). Screening these disruption strains for a cold-sensitive growth phenotype we identified *YVH1*, encoding a dual-specificity protein phosphatase related to vaccinia virus VH1. The absence of Yvh1 caused a growth defect at 30°C and a severe growth defect at 13°C, while disruption of other protein phosphatases did not impair normal growth at these temperatures (*2*).

In *S. cerevisiae* Yvh1 has not only been implicated in the regulation of vegetative growth, but also in glycogen metabolism, ribosome biogenesis, and sporulation. Nitrogen starvation in the absence of a fermentable carbon source causes diploid cells to undergo meiosis resulting in the production of haploid spores. Loss of Yvh1 decreases, but does not abolish, expression of early meiotic regulators, like the master sporulation regulator *IME1* and its target *IME2* (*4*). Yvh1 acts upstream of Mck1, a dual-specificity protein kinase that varies the level of *IME1* expression in response to nutritional signals, as over-expression of *MCK1* or *IME1* rescued the sporulation defect occurring in absence of Yvh1 (*4*, *5*). Glycogen metabolism is another process affected upon disruption of *YVH1*: accumulation of glycogen as observed for wild-type cells going into stationary phase was not observed in absence of Yvh1 (*6*). Furthermore, there are indications that Yvh1 is involved in ribosome biogenesis: two-hybrid analysis demonstrated that Yvh1 physically interacts with Nop7/Yph1 (Yeast Pescadillo Homologue) (*7*, *8*), which turned out to be a nucleolar protein associated with pre-60S particles (*9*) to support their transport and assembly (*10*). Depletion of Nop7 also causes a defect in the processing of 25S precursors (*10*). Moreover,

Yvh1 was recently reported to be a novel ribosome assembly factor (*11*) required for the release of Mrt4, a ribosomal stalk protein Rpp0 paralogue involved in mRNA turnover and ribosome biogenesis (*9*, *12*), from cytoplasmic pre-60S particles to enable loading of the ribosomal stalk protein Rpp0 (*13*, *14*). How can Yvh1 be involved in so many different processes?

In this study, we have isolated mutants capable of suppressing the slow-growth phenotype of the *Δyvh1* disruptant. One of the suppressor-alleles, *SVH1-1,* we found to be a dominant mutant allele of *MRT4* that results in an amino acid change from Gly^{68} to Asp [*MRT4(G68D)*] which enables the mutant Mrt4 to restore the growth-defect phenotype of the *Δyvh1* strain. Although same and similar mutations were recently reported independently by Lo *et al.* (*13*) and Kemmler *et al.* (*14*) as a mutation that can suppress the defective maturation of 60S ribosomal particles caused by the absence of Yvh1, we show here that *MRT4(G68D)* mutation restores, apart from normal growth and rRNA maturation, also the other phenotypes that occur in absence of Yvh1, including a delay in mRNA turnover and defects in glycogen accumulation and sporulation. We found that recovery of sporulation efficiency in *Δyvh1 MRT4(G68D)* diploids was accompanied by up-regulation of early meiotic genes which are down-regulated in the *Δyvh1* disruptant. The expression level of *IME1* was not affected by absence of Yvh1 although genes activated by its translation product were. Since a defect in ribosome biogenesis in general can be related to other various defects (*4*, *6*, *12*, *15–19*), the ribosome biogenesis defect caused by absence of Yvh1 might be an indirect cause of observed phenotypes.

Experimental Procedures

Strains and media

The *S. cerevisiae* wild-type strains used in this study were W303-1A (SH4848, *MAT***a** *ura3-1 leu2-3, 112 trp1 his3-11, 15 ade2-1*), W303-1B (SH4849, *MATα ura3-1 leu2-3, 112 trp1 his3-11, 15 ade2-1*) (*20*), and their diploid, W303 (SH4502). The *Δyvh1* disruptants were made in W303-1A (SH7783, *Δyvh1*::*CgTRP*) and W303-1B (SH6001, *Δyvh1*::*CgHIS3*) (*3*). SVH1-1 mutant (SH6002) was isolated as a suppressor of the slow growth of *Δyvh1* (SH6001). All strains were propagated on YPDA medium [1% yeast extract, 2% peptone, 2% glucose (Sigma-Aldrich, St Louis, MO, USA), and 0.04% adenine] or synthetic complete (SC)-ura medium [2% glucose, 0.67% yeast nitrogen based without amino acids (Becton, Dickinson and Company, Sparks, MD, USA), and the required auxotrophic supplements without uracil]. All solid media contained 2% agar. For sporulation, we constructed diploid strains homozygous for *Δyvh1* and heterozygous for *MRT4(G68D)* by crossing SH7783 and SH6001, and SH7783 and SH6002. Cells were pre-grown in YEPAc (2% polypeptone, 1% yeast extract, and 2% potassium acetate) at 30°C to a density of OD_{660} ~1.0, washed twice with sporulation medium (2% potassium acetate, pH 6.6), and resuspended in pre-warmed and pre-aerated sporulation medium to an OD_{660} ~1.0. The cultures were then incubated at 30°C for 6–12 h before mRNA-levels were determined by real-time polymerase chain reaction (PCR) (see below) and for over 6 days the numbers of asci were counted.

Analysis of Δyvh1 suppressors

The *Δyvh1* disruptant SH6001 was mutagenized with ethyl methanesulfonate according to standard procedures (*21*) and grown on YPDA plates at 30°C, replica-plated onto two fresh YPDA plates and kept at 13°C and 30°C yielding 28 fast growing colonies, which contained dominant suppressors of *Δyvh1*, *SVH1*. From one of these, *SVH1-1* (SH6002), a chromosomal DNA library was constructed by cloning its genomic DNA, partially digested with HindIII (Takara Bio, Kyoto, Japan), into pMO36 (*tet*^{r}, *URA3*, ARS/CEN), a derivative of pTR262 (*22*), and transformed into *Δyvh1* strain SH6001. Plasmids from fast-growing transformants were verified to be able to suppress the slow growth of *Δyvh1* at 30°C and 13°C after retransformation of *Δyvh1* strain SH6001. Candidates were analysed by restriction digests and sequencing. Subclones were prepared from one of these plasmids, pSANS4, and from these only pSANS4MRT2, containing a 3.2 kb XbaI and EcoRV fragment in pRS316 (Fig. 2A) showed to have *SVH1-1* activity. The responsible gene had to be *MRT4*, the only gene absent from other non-complementing plasmids, which was confirmed by testing plasmids pSANMRTWT-1 and pSANMRTSV-1 that contained, respectively, wild-type and mutant versions of *MRT4* (including 0.41 kb upstream and 0.39 kb downstream sequence) amplified by PCR (using primers MRT4-1 and MRT4-2, Table I) from wild-type W303-1B or SVH1-1 (SH6002) genomic DNA and cloned into pRS316 as BamHI–SalI fragments. The mutation of

Table I. Oligonucleotides used in this study.

Name	Sequence (5′–3′)
MRT4-1	CTCGTCGACGCTATGGGACTCATGTTCATCAAGGT
MRT4-2	CTCGGATCCCACTACTCCAACTGACAGTACTCCAA
IME2-RT1	GATGCCAGTAATTTGGTCCATAAA
IME2-RT2	TGACAACCTCAGATAAATCGGATAGT
IME1-RT1	GCAAGCGGATATGCATGGA
IME1-RT2	TGCTGTTCAAAAGGAAAGAGGAA
SPO13-RT1	CGCCCCTCATTTGATAATTCC
SPO13-RT2	GAACCGGCGTTGAAGTAGATTT
HOP1-RT1	CCCAGTCACGGGCATTTG
HOP1-RT2	ACACGGTGGCTGCTTTGG
ACT1-RT1	TCGAGAGATTTCTCTTTTAC
ACT2-RT2	TCTGGGGCTCTGAATCTTTC
RPL28-1	ATGCCTTCCAGATTCACTAA
RPL28-2	TTAAGCGATCAATTCAACAA
URA5-1	ATGCCTATTATGTTGGAAGA
URA5-2	TTAAGCGGAGGCACCGTAGG
35S-3	AAGAAATTTAATAATTTTGAAAATGGATTT
35S-5	GTTGTATTGAAACGGTTTTAATTGTCCTAT
35S-7	AAACTTTCAACAACGGATCTCTTGGTTCTC
35S-8	TTTAAGAACATTGTTCGCCTAGACGCTCTC

Restriction enzyme sites are underlined.

SVH1-1 (SH6002) was determined by comparing the sequenced inserts of pSANMRTWT-1 and pSANMRTSV-1 as well as of five independent pUC19 clones containing the *MRT4* fragment amplified with primers MRT4-1/-2 from SVH1-1 (SH6002) genomic DNA.

Integration mapping

Plasmid pSANI-1, which is SmaI/XbaI cut pRS306 (*amp*^{r}, *URA3*; *23*) ligated to the EcoRV/XbaI fragment from pSANS4, was linearized by cleavage within the mutant *MRT4* and transformed into SVH1-1 strain SH6002. Stable Ura$^+$ transformants were isolated and the correct integration of the plasmid into the *MRT4* locus was verified by southern blot analysis. The obtained strain was mated with *Δyvh1* (SH7783) and, after tetrad analysis, growth of spores was monitored at 30°C on YPDA plates and checked for 2:2 Ura$^+$ Svh$^+$:Ura$^-$ Svh$^-$ segregation, indicative for genetic linkage.

Glycogen staining

Glycogen was detected after 1×10^4 cells were spotted onto SC plates, incubated for 4 days at 30°C and exposed to iodine vapour as described (*24*).

Measurement of mRNA decay rates

As described previously (*25*), 50 ml cultures in YPDA medium were grown to mid-log phase, collected by centrifugation, resuspended in 12 ml of pre-warmed fresh medium and shaken at 30°C. Transcription was then inhibited by the addition of thiolutin (Tocris Bioscience, Bristol, UK) to a final concentration of 20 μg/ml, and 2 ml aliquots were snap-frozen after 0, 5, 10, 15, 20 and 35 min. RNAs from these samples were isolated and analysed by northern blotting as described below and hybridized to *RPL28* and *URA5* mRNA probes prepared by PCR with primers RPL28-1/ RPL28-2 and URA5-1/ URA5-2, respectively (Table I). The half-lives were determined by calculating mRNA band intensity using Labo-1D software (KURABO, Tokyo) and normalization of the data such that time zero after addition of thiolutin equalled 100%.

RNA isolation, cDNA preparation, quantitative real-time PCR and northern blot analysis

Total RNAs were isolated as described (*26*). For the preparation of cDNA extracted RNAs were treated with DNase I (Nippon gene, Tokyo, Japan) and reversely transcribed using QuantiTech Reverse Transcription kit (Qiagen, Valencia, CA, USA) according to the manufacturer's instructions. Quantitative real-time PCR was performed using SYBR green PCR Master Mix (Applied Biosystems, Foster City, CA, USA) in triplicates in an Applied Biosystems 7300 real-time PCR system (Applied Biosystems, Foster City, CA, USA) according to the manufacturer's instructions. Relative mRNA levels were normalized to *ACT1* mRNA levels. For determination of mature rRNA levels by real-time PCR total RNA isolated from 10 ml of yeast cultures, grown to mid-log phase in selective media, was used. For northern blot analysis, RNAs (20 μg) were resolved on 2.0% agarose–formaldehyde gel, stained with ethidium bromide to visualize 25S and 18S species, and transferred to Hybond N$^+$ membrane (GE Healthcare Bio-Science Corp., Piscataway, NJ, USA). The Alkphos Direct Labeling and Detection System (GE Healthcare Bio-Science Corp.) was used for probe labelling, hybridization and detection; blots were exposed on ECL film (GE Healthcare Bio-Science Corp.). Primers used for quantitative real-time PCR, e.g. to determine mRNA levels for *ACT1* (ACT1-RT1/ACT1-RT2), *IME2* (IME2-RT1/IME2-RT2), *IME1* (IME1-RT1/IME1-RT2), *SPO13* (SPO13-RT1/SPO13-RT2) and *HOP1* (HPO1-RT1/HOP1-RT2), and to prepare probes for northern blot analysis are listed in Table I. Probes I and II used for the detection of pre-RNAs were prepared by PCR using two primer sets, 35S-3/35S-5 and 35S-7/35S-8, respectively. Probe II was used to detect mature 5.8S rRNA. For normalization of pre-rRNA intensities, blots were stripped and reprobed for *ACT1* as a loading control. To calculate total RNA (mg)/OD_{660} ratios, the amounts of total RNA isolated from cells grown to mid-log phase ($OD_{660} = \sim 1.0$) in 50 ml of YPDA were determined by measuring the absorbance at 260 nm and divided by the OD_{660} values of the corresponding cultures.

Results

A mutation in Mrt4 suppresses the growth defect of Δyvh1

Strains in which Yvh1 is absent grow slowly at all temperatures (Fig. 1A; *2–6*, *8*, *11*, *13*, *14*, *27*), have a sporulation defect and do not accumulate glycogen during stationary phase (Fig. 4A; *4–6*, *8*), which can be suppressed by expression of the C-terminal region of the protein but not its catalytic centre (*6*, *27*). The exact mechanism by which Yvh1 acts during sporulation and glycogen accumulation is not known and in order to enhance the understanding of its role, we set out to isolate suppressors of the *Δyvh1* growth defect. We undertook ethyl methanesulfonate mutagenesis of the *Δyvh1* disruptant and obtained 28 colonies capable of growing faster at 13°C and 30°C. Standard genetic analysis performed on the suppressors, termed *SVH1* (suppressor of *Δyvh1* deletion), showed that they were allelic and dominant.

Genomic DNA isolated from one of those suppressors, SVH1-1, was used to construct a library from which 31 plasmids were isolated that suppressed the growth defect of the *Δyvh1* disruptant. Restriction analysis and sequencing showed that these plasmids carried the same HindIII inserts, one of which derived from chromosome XIII and the other two from one locus on chromosome XI, indicating that two

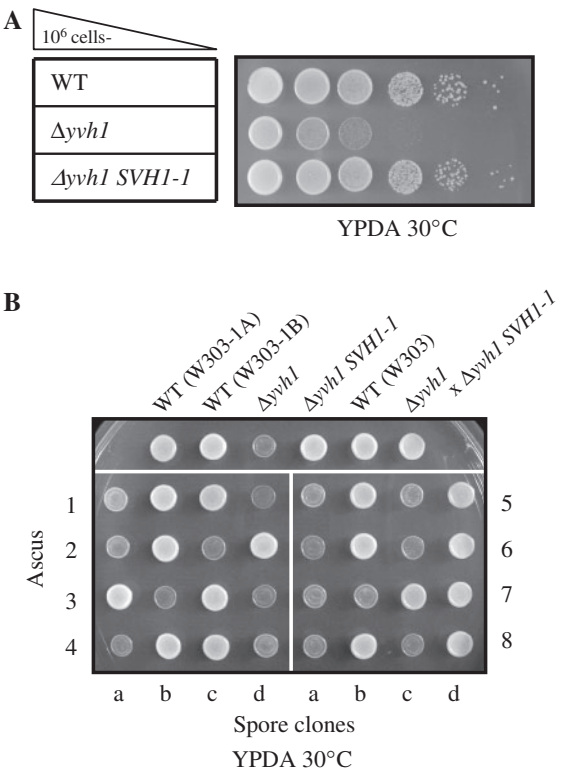

Fig. 1 Suppression of the *Δyvh1* growth-phenotype by *SVH1-1*. (A) 10-fold dilutions of wild-type yeast (WT; SH4849), *Δyvh1* (SH6001) and *Δyvh1 SVH1-1* (SH6002) cells were spotted on YPDA medium and incubated at 30°C. (B) Tetrad analysis of the diploid resulting from a cross between *Δyvh1 SVH1-1* (SH6002) and *Δyvh1* (SH7783). Each dissected ascus is numbered and small letters indicate its spores.

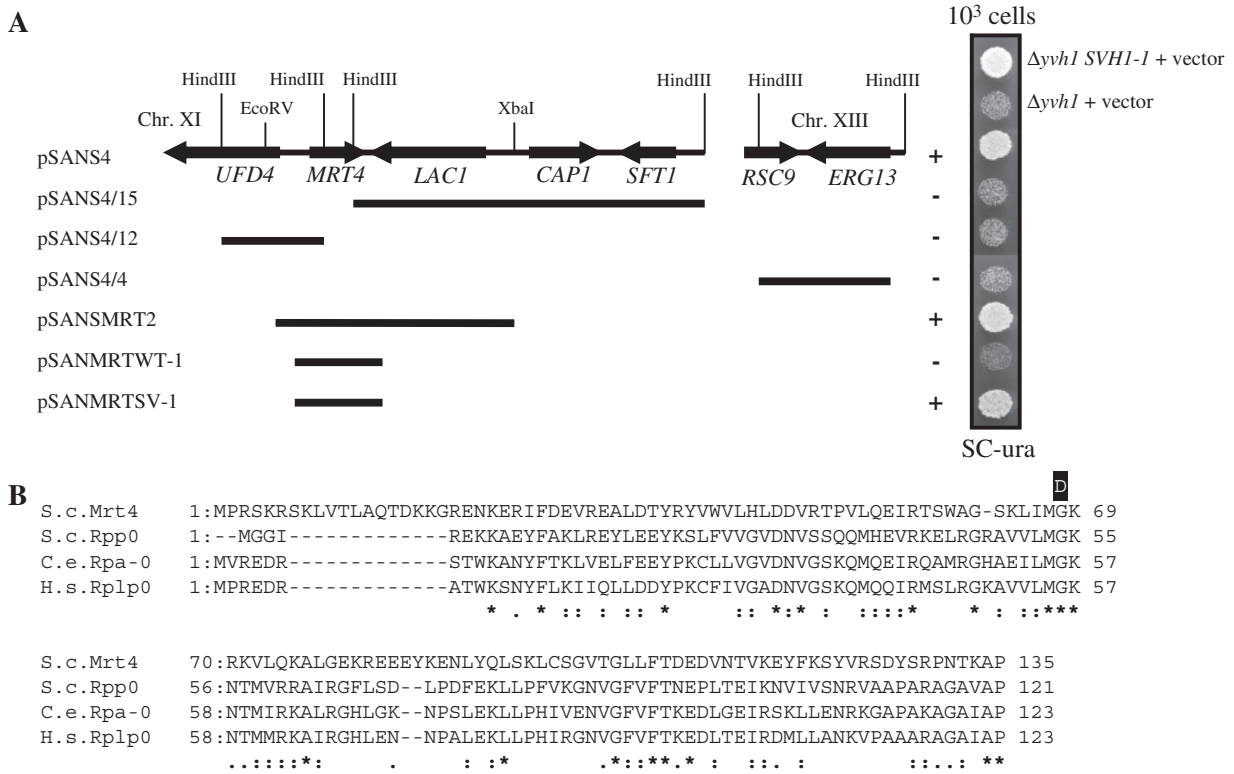

Fig. 2 Complementation tests (A) and amino-acid change on Mrt4 (B). (A) After transformation of *Δyvh1 SVH1-1* (SH6002) with pMO36 (vector), or *Δyvh1* (SH6001) with pMO36 (vector), pSANS4, or pRS316 containing the indicated fragments sub-cloned from pSANS4 (pSANS4/15, /12, /4, MRT2) or PCR amplified wild-type (pSANMRTWT-1) and mutant *MRT4* genes (pSANMRTSV-1), cells were spotted on SC-ura medium and grown at 30°C for 2 days. The plus and minus signs indicate complementation or lack thereof, respectively, of the *Δyvh1* disruptant. (B) ClustalW2 (http://www.ebi.ac.uk/) alignment of *S. cerevisiae* Mrt4 and Rpp0 and *C. elegans* and *H. sapiens* Rpp0 homologs. Conserved amino acids are indicated with an asterisk below the alignment; '–' represents gaps, ':' indicate conserved substitutions and '.' semi-conserved substitutions. The G68D mutation (D) is indicated above the sequence.

fragments had been ligated into the same vector, yielding plasmid pSANS4 (Fig. 2A). Complementation analysis with subclones derived from this plasmid identified *MRT4* (for mRNA turnover; *12*) as the gene harbouring the *SVH1-1* allele. A subclone pSANS4MRT2 was the only plasmid other than pSANS4 that complemented the *Δyvh1* disruptant and contained the complete coding sequence of *MRT4* including its putative promoter and terminator regions (Fig. 2A). This was confirmed by the finding that the *MRT4* gene isolated by PCR from SVH1-1 was able to suppress the *Δyvh1* growth defect, whereas the wild-type copy did not complement (Fig. 2A). Furthermore, upon integration of *URA3* into the *MRT4* locus of SVH1-1 and subsequent analysis of 14 tetrads, we found that the marker co-segregated with *SVH1-1* suppressor activity (data not shown), demonstrating genetic linkage and that SVH1-1 harbours a dominant *MRT4* allele.

When the coding sequence of *MRT4* isolated from the SVH1-1 suppressor was compared to that of the parental strain, only a single-nucleotide substitution was found, namely a change from G to A at position 202 of *MRT4*. Mrt4 has 44% similarity to ribosomal protein Rpp0, a central component of the *S. cerevisiae* ribosomal stalk complex (*28*). The N-terminal region of Rpp0 is highly conserved in eukaryotes, and 121 amino acids in this region are directly involved in the interaction of Rpp0 with the ribosomal RNA (rRNA) (*29*). Interestingly, a similar N-terminal region is present in Mrt4 and the *MRT4* mutation we identified in this study changed an evolutionarily conserved glycine at position 68 in this domain to an aspartic acid (Fig. 2B). Hereafter, we describe the *SVH1-1* mutation as *MRT4(G68D)*.

Yvh1 is involved in normal accumulation of rRNAs

A same and similar *MRT4* mutation was recently reported independently by Lo *et al.* (*13*) and Kemmler *et al.* (*14*) as a dominant mutation that can suppress the defective maturation of 60S ribosomal particles caused by the absence of Yvh1. When we examined steady-state levels of mature ribosomal RNAs (Fig. 3A and B) by northern analysis, we observed that the absence of Yvh1 leads to reduced steady-state levels of both the small subunit 18S rRNA and the large subunit 25S and 5.8S rRNAs. Especially the amount of 25S rRNA decreased, to ~40–60% of wild-type levels, whereas the abundance of 18S (60–80%) and 5.8S (80%) rRNAs was less affected (Fig. 3B). In line with this, the total amount of RNA in *Δyvh1* cells was <60% of wild-type cells (Fig. 3C), indicating that, as the majority of RNA in the cell is ribosomal,

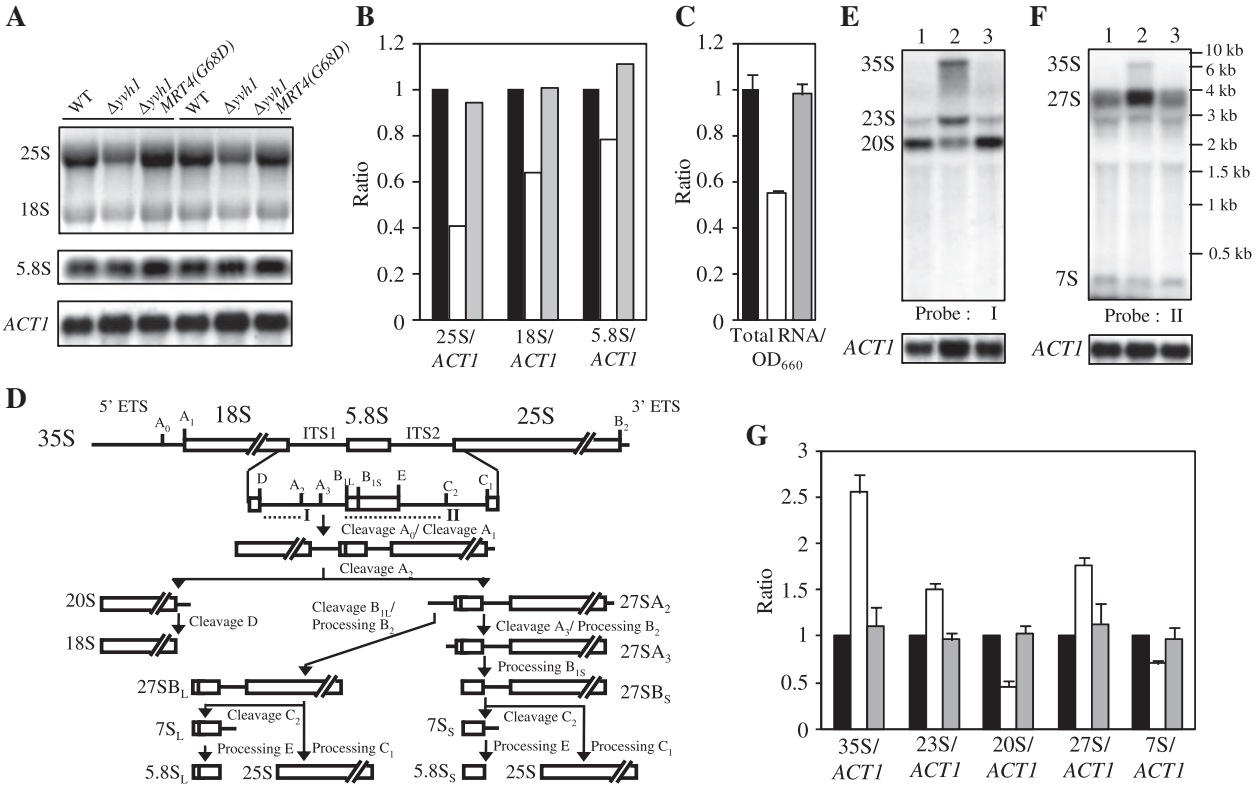

Fig. 3 Steady-state levels of mature rRNA species and analysis of pre-rRNA processing. (A) After ethidium bromide staining (top panel) northern blots of total RNA from wild-type (SH4849), *Δyvh1* (SH6001), and *Δyvh1 MRT4(G68D)* (SH6002) strains were probed for 5.8S rRNA as described in the Experimental Procedures, stripped and reprobed for *ACT1* as a control (lower panels). Two sets of experiments using independent samples are shown and (B) used to obtain normalized averages of relative levels of the mature rRNAs. Black, white, and grey bars indicate wild-type, *Δyvh1*, and *Δyvh1 MRT4(G68D)* strains, respectively. (C) Assessment of total RNA. Ratios of total RNA (μg) to OD_{660} of cultures determined from three independent experiments (including the standard deviations) as described in the 'Experimental Procedures' section are depicted. Black, white, and grey bars indicate wild-type, *Δyvh1*, and *Δyvh1 MRT4(G68D)* strains, respectively. (D) Major pre-rRNA processing pathway in *S. cerevisiae*. In the 35S pre-rRNA the mature 18S, 5.8S, and 25S rRNA sequences are flanked by the 5′ and 3′ external transcribed spacers (ETS) and separated by internal transcribed spacers 1 and 2 (ITS1 and ITS2). Pre-rRNA cleavage sites are indicated by upper-case letters. The positions of probes used for northern blotting are indicated as I and II by dotted lines. (E and F) Total RNAs prepared from wild-type (SH4849, lane 1), *Δyvh1* (SH6001, lane 2), and *Δyvh1 MRT4(G68D)* (SH6002, lane 3) strains were analysed by northern blotting with probes I (E) and II (F). Positions of pre-rRNA species and size markers are indicated on the left and right side of each panel. (G) Values for pre-rRNA levels were normalized to that of *ACT1* and expressed relative to those of the wild-type strain (defined as 1.0); error bars show the standard deviation of three independent experiments. Black, white, and grey bars indicate wild-type, *Δyvh1*, and *Δyvh1 MRT4(G68D)* strains, respectively.

the growth defect in the absence of Yvh1 could be caused by a defect in ribosome synthesis.

The production of the mature ribosomal RNAs occurs by processing of a 35S precursor RNA, which is assembled with ribosomal proteins and processing factors into a large complex (*30*). Cleavages at sites A0, A1, and A2 generate the 20S and 27S precursors of, respectively, the small and large subunit rRNAs (Fig. 3D). Subsequent processing of 27S pre-rRNA occurs at sites A3 and B1 to generate the 5′-end of 5.8S rRNA and at C1 and C2 to remove the second internal transcribed spacer (ITS2) separating the 5.8S and 25S sequences. In absence of Yvh1, the early processing at A0, A1 and A2 is compromised as the 35S pre-rRNA accumulated about 2.5-fold whereas an aberrant 23S product, which presumably resulted from cleavage at A3 or B1 (*30*), becomes 1.5-fold more abundant (Fig. 3E and G). Concomitantly, 2-fold less 20S pre-rRNA is formed by processing at A2 than in case of the wildtype. The 27S large subunit pre-rRNA that is generated in *Δyvh1* cells together with the 20S and 23S species accumulated >1.5-fold (Fig. 3F and G), indicating that the subsequent removal of ITS2 is affected. This could explain the low 25S rRNA levels described above and is supported by the 20% reduced steady-state level of the 7S precursor of 5.8S rRNA which is formed by cleavage at C2 (Fig. 3F and G). Thus, Yvh1 is involved in both early as well as late pre-rRNA processing steps. Its absence seems to have a major impact on the late steps that generate mature 25S rRNA leading to less 60S subunits that also could be functionally impaired. As a result, the number and quality of ribosomes formed in *Δyvh1* cells could be insufficient to support normal growth.

MRT4(G68D) *restores glycogen accumulation and sporulation in Δ*yvh1

Disruption of *YVH1* causes a defect in glycogen accumulation and sporulation (*4–6*, *8*). This prompted us to examine whether the *MRT4(G68D)* mutation that virtually alleviates the shortage of mature rRNAs in

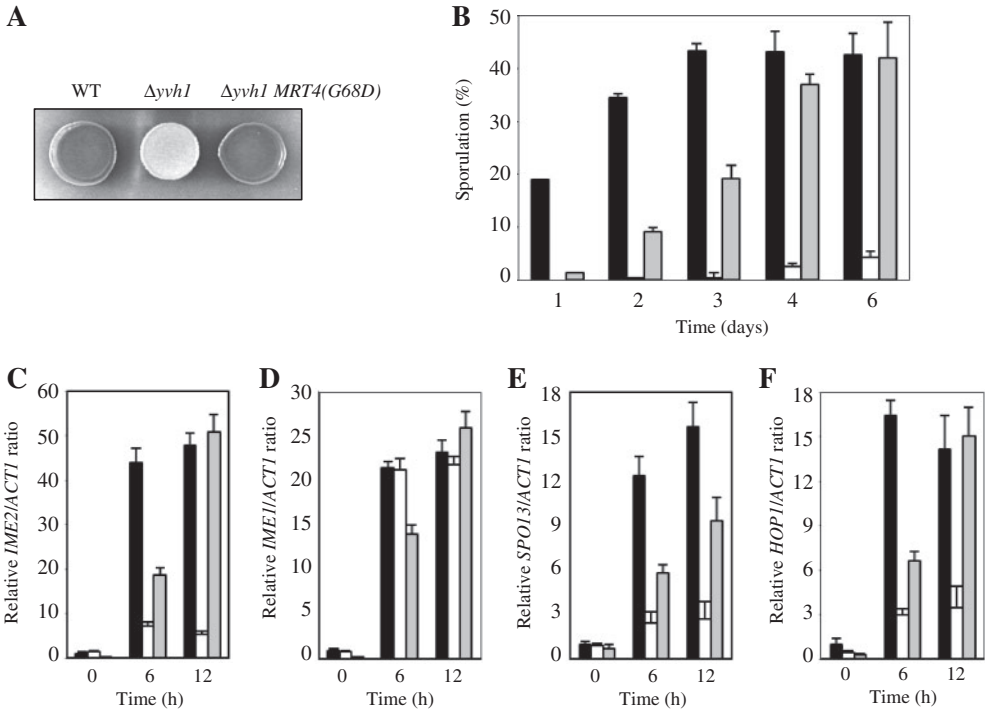

Fig. 4 Glycogen staining, sporulation efficiency, and *IME2*, *IME1*, *SPO13*, and *HOP1* transcription levels. (A) Glycogen accumulation in wild-type (SH4849), *Δyvh1* (SH6001), and *Δyvh1 MRT4(G68D)* (SH6002) cells was visualized by iodine staining as described in the 'Experimental Procedures' section. (B) Upon transfer to sporulation medium (Experimental Procedures) wild-type (black bars), *Δyvh1*/*Δyvh1* (white bars), and *Δyvh1*/*Δyvh1 MRT4*/*MRT4(G68D)* (grey bars) cultures were sampled at indicated time points and monitored by light microscopy. The graph shows the percentages of asci observed among at least 300 cells. (C–F) The mRNA levels of *IME2* (C), *IME1* (D), *SPO13* (E), and *HOP1* (F) were analysed in wild-type (black bars), *Δyvh1*/*Δyvh1* (white bars), and *Δyvh1*/*Δyvh1 MRT4*/*MRT4(G68D)* (grey bars) diploid cells grown in sporulation medium by quantitative real-time PCR. Relative mRNA values (normalized to *ACT1* expression) determined in triplicate are indicated with wild-type values at time 0 set to 1.0; the error bars show the standard deviation.

Δyvh1 cells could also repair the glycogen accumulation defect. In agreement with a previous report (*6*), *Δyvh1* cells failed to accumulate glycogen relative to the wild-type cells as indicated by the lack of brown colorization after iodine staining (Fig. 4A). In contrast, *Δyvh1 MRT4(G68D)* cells appeared to accumulate glycogen to wild-type levels.

To test whether *MRT4(G68D)* mutation also suppresses the spoluration deficiency of the *Δyvh1* disruptant, we constructed diploid strains homozygous for *Δyvh1* and heterozygous for *MRT4(G68D)*. The sporulation efficiency of these strains and those of homozygous *Δyvh1* and wild-type diploids were compared by determining the number of tetrads formed over time in each diploid (Fig. 4B). In the homozygous *Δyvh1* culture, 4% asci could be counted after 6 days of sporulation. In contrast, the number of asci formed from wild-type cells after 3 days and from homozygous *Δyvh1* cells heterozygous for *MRT4(G68D)* after 6 days was 10-fold higher: ~40% spore-forming cells were counted. Thus, apart from defects in growth, ribosome biogenesis, and glycogen formation, the *MRT4(G68D)* mutation also suppressed the sporulation defects of the *Δyvh1* disruptant.

Mrt4(G68D) reinstates the expression of early meiotic genes IME2, SPO13 *and* HOP1 *in Δ*yvh1 *cells*

Decreased sporulation efficiency in *Δyvh1* cells is accompanied by dramatically reduced expression of the early meiotic gene *IME2* which encodes a Ser/Thr protein kinase and is a positive regulator of early, middle and late meiotic genes (*4*). To gain more insight into the molecular mechanisms by which the *MRT4(G68D)* suppresses the sporulation defect of *Δyvh1* cells, we examined by quantitative real-time PCR the expression levels of *IME2* after induction of sporulation in diploid wild-type, homozygous *Δyvh1*, and homozygous *Δyvh1* cells heterozygous for *MRT4(G68D)* (Fig. 4C). After 6 h of transfer to sporulation medium *IME2* expression in wild-type diploid cells increased to ~40-fold higher levels than that of actin mRNA. In contrast, such induction was absent from homozygous *Δyvh1* cells even after 12 h in sporulation medium, confirming the previously reported result (*4*). When homozygous *Δyvh1* cells heterozygous for *MRT4(G68D)* were transferred to sporulation medium, *IME2* mRNA levels increased to the same level as wildtype after 12 h, indicating that expression of *IME2* in the *Δyvh1* disruptant is restored by the *MRT4(G68D)* mutation.

Expression of *IME1*, which encodes a positive regulator of *IME2*, has been reported to be 2-fold lower than wildtype after 6 h incubation in sporulation medium (*4*). We did not, however, observe such a decrease in *IME1* expression in homozygous *Δyvh1* cells (Fig. 4D). In contrast, in these cells we found that expression of *SPO13* and *HOP1*, both of which are early meiotic genes transactivated by Ime1, are

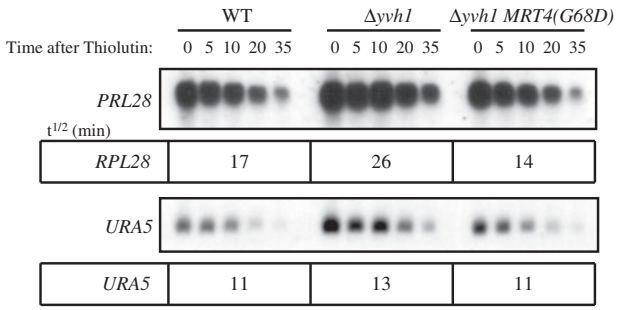

Fig. 5 Analysis of mRNA decay. Wild-type (SH4849), *Δyvh1* (SH6001), and *Δyvh1 MRT4(G68D)* (SH6002) strains were grown to mid-log phase, and then incubated with 20 μg/ml thiolutin. The half-lives (min) of *RPL28* (top) and *URA5* (bottom) mRNAs shown below each northern blot were determined as described in the 'Experimental Procedures' section.

down-regulated. Upon introduction of Mrt4(G68D) in the absence of Yvh1 *SPO13* was up-regulated more than three times while expression of *HOP1* increased 5-fold and reached wild-type levels after 12 h in sporulation medium (Fig. 4E and F). These results indicate that the *MRT4(G68D)* mutation enhanced the expression of early meiotic genes that were not significantly induced in the *Δyvh1* disruptant upon transfer to sporulation medium. Thus, the efficient sporulation we observed for diploid *Δyvh1 MRT4(G68D)* cells probably results from the partial recovery of wild-type regulation of early meiotic genes in these cells. This would further suggest that disruption of *YVH1* may cause some defects downstream of *IME1* transcription.

Disruption of YVH1 moderately increases half-lives of mRNAs

MRT4 has not only been identified as a component of a pre-ribosomal particle (*9*, *13*, *14*) but also in a screen for factors involved in mRNA decay (*12*). Mutant *mrt4-1189* containing an A to G change at position 647, which results in a change of lysine 216 to arginine in Mrt4, caused a temperature-sensitive phenotype. At 37°C the *mrt4-1189* mutant exhibited a 2- to 3-fold increase in the half-lives of *RPL28* and *URA5* mRNAs. Accordingly, incomplete absence of Mrt4 the *URA5* mRNA became 3-fold more stable (*12*). Disruption of *MRT4* causes a general growth defect (*9*, *13*, *14*), presumably because Mrt4 is required for proper nuclear export of pre-60S ribosomal particles (*13*, *14*).

Since *MRT4* appears to be involved in mRNA turnover, we examined whether Yvh1 also functions in mRNA decay by analysing the kinetics of turnover of *RPL28* and *URA5* mRNAs in the wild-type, *Δyvh1*, and *Δyvh1 MRT4(G68D)* cells. The *URA5* mRNA has a short half-life while the *RPL28* mRNA is a moderately stable transcript (*31*). Northern blot analyses from which the half-lives of the *RPL28* and *URA5* mRNAs were calculated are shown in Fig. 5. In the absence of Yvh1, the decay rates of *RPL28* and *URA5* mRNAs moderately decreased compared to the rates measured for the wild-type strain, leading to 1.5- and 1.2-fold increases in the half-lives of these mRNAs, respectively. Interestingly, introduction of the *MRT4(G68D)* allele into the *Δyvh1* disruptant resulted in shorter half-lives for both mRNAs tested. The stability of the *URA5* mRNA returned to that of wild-type, whereas the *RPL28* transcripts appeared to be degraded even faster than normal, indicating that Mrt4(G68D) accelerates mRNA turnover in *Δyvh1* cells. These results show that Yvh1 is, directly or indirectly, involved in mRNA turnover.

Discussion

In this study, we isolated a *MRT4(G68D)* mutation as a suppressor of the slow growth phenotype of a *Δyvh1* disruptant. Our analysis revealed that *Δyvh1* cells failed to accumulate mature rRNAs, especially 25S rRNA and, to a lesser extent, 18S and 5.8S rRNAs (Fig. 3B), which was accompanied by delayed processing of 35S and 27S pre-rRNAs (Fig. 3G). Especially the late maturation steps involving the removal of the ITS2 appeared to be affected, leading to a reduction of mature 25S rRNA by over 60%. These ribosome biogenesis defects were, however, absent when Mrt4(G68D) was expressed in these cells, indicating that absence of Yvh1 has been compensated by a single amino acid change in the N-terminal region of Mrt4 highly similar to the rRNA binding region of the essential ribosomal stalk protein Rpp0 (Fig. 2B). Interestingly, Mrt4p and Rpp0 association with 25S rRNA is mutual exclusive, while a chimaeric protein consisting of the N-terminal rRNA binding domain of Mrt4 and the C-terminal region of Rpp0 can complement for the absence of Rpp0 although its association with the small subunit appears to be weaker. (*32*). Very recently, Yvh1 was reported to be a novel ribosome assembly factor (*11*) required for the release of Mrt4 from cytoplasmic pre-60S particles to enable loading of the ribosomal stalk protein Rpp0 (*13*, *14*). It was shown that Yvh1 is essential for a late maturation step in the 60S biogenesis and that disruption of *YVH1* causes a rRNA processing delay, which is consistent with our findings.

Importantly, we found that the *MRT4(G68D)* mutation not only restores growth of *Δyvh1* cells and normal accumulation of mature rRNAs in these cells, but rescued all other *Δyvh1* phenotypes tested, i.e. defects in sporulation and glycogen accumulation as well as reduced mRNA turnover (Figs 4 and 5), not described in any other studies on Yvh1/Mrt4 cooperation. As far as we know, many gene including *NUP120*, *RPL35A*, and *RRP4*, that are involved in ribosome biogenesis, are reported to show defects, when disrupted or conditionally repressed, in glycogen accumulation, sporulation, or mRNA catabolic process (*4*, *6*, *12*, *15–19*). Furthermore, disruption or conditional repression of a lot of genes involved in ribosome biogenesis, which causes ribosome biogenesis defects such as decreased accumulation of 40S or 60S ribosome subunits, also causes other various defects including increased heat and cold sensitivity, decreased resistance to many drugs, or abnormal morphology of mitochondria (*Saccharomyces* Genome Database: http://www.yeastgenome.org). Although their detailed

mechanisms are not clear, it is possible to speculate that a defect in ribosome biogenesis, in general, can be related to other various defects, and thus loss of Yvh1 that likely causes impaired ribosome biogenesis results in multiple phenotypes including glycogen accumulation, sporulation, and mRNA decay defects. Therefore, these data suggest that fairly different phenotypes of *Δyvh1* cells may be caused by a diminished accumulation of fully functional ribosomes occurring in the absence of Yvh1 (*11*, *13*, *14*).

Human *YVH1* was frequently amplified and highly expressed in sarcomas (*33*). Over-expression of human *YVH1* during sarcoma development or progression would correlate with up-regulation of ribosome biogenesis during tumourigenesis and proliferation of tumour cells (*34*). Since human Yvh1 is also able to release Mrt4 in human cells (*13*), we think that human Yvh1 is involved in sarcoma development through ribosome biogenesis.

Funding

Ministry of Education, Culture, Sports, Science and Technology, a Grant-in-Aid for Scientific Research B, 19380193, 2007 to 2009 (to S.H.).

Conflict of interest

None declared.

References

1. Zolnierowicz, S. and Bollen, M. (2000) Protein phosphorylation and protein phosphatases De Panne, Belgium. *EMBO J.* **19**, 483–488
2. Sakumoto, N., Mukai, Y., Uchida, K., Kouchi, T., Kuwajima, J., Nakagawa, Y., Sugioka, S., Yamamoto, E., Furuyama, T., Mizubuchi, H., Ohsugi, N., Sakuno, T., Kikuchi, K., Matsuoka, I., Ogawa, N., Kaneko, Y., and Harashima, S. (1999) A series of protein phosphatase gene disruptants in *Saccharomyces cerevisiae*. *Yeast* **15**, 1669–1679
3. Sakumoto, N., Matsuoka, I., Mukai, Y., Ogawa, N., Kaneko, Y., and Harashima, S. (2002) A series of double disruptants for protein phosphatase genes in *Saccharomyces cerevisiae* and their phenotypic analysis. *Yeast* **19**, 587–599
4. Park, H.D., Beeser, A.E., Clancy, M.J., and Cooper, T.G. (1996) The *S. cerevisiae* nitrogen starvation-induced Yvh1 and Ptp2p phosphatases play a role in control of sporulation. *Yeast* **12**, 1135–1151
5. Beeser, A.E. and Cooper, T.G. (1999) The dual-specificity protein phosphatase Yvh1 acts upstream of the protein kinase Mck1p in promoting spore development in *Saccharomyces cerevisiae*. *J. Bacteriol.* **181**, 5219–5224
6. Beeser, A.E. and Cooper, T.G. (2000) The dual-specificity protein phosphatase Yvh1 regulates sporulation, growth, and glycogen accumulation independently of catalytic activity in *Saccharomyces cerevisiae* via the cyclic-AMP-dependent protein kinase cascade. *J. Bacteriol.* **182**, 3517–3528
7. Kinoshita, Y., Jarell, A.D., Flaman, J.M., Foltz, G., Schuster, J., Sopher, B.L., Irvin, D.K., Kanning, K., Kornblum, H.I., Nelson, P.S., Hieter, P., and Morrison, R.S. (2001) Pescadillo, a novel cell cycle regulatory protein abnormally expressed in malignant cells. *J. Biol. Chem.* **276**, 6656–6665
8. Sakumoto, N., Yamashita, H., Mukai, Y., Kaneko, Y., and Harashima, S. (2001) Dual-specificity protein phosphatase Yvh1, which is required for vegetative growth and sporulation, interacts with yeast Pescadillo homologue in *Saccharomyces cerevisiae*. *Biochem. Biophys. Res. Comm.* **289**, 608–615
9. Harnpicharnchai, P., Jakovljevic, J., Horsey, E., Miles, T., Roman, J., Rout, M., Meagher, D., Imai, B., Guo, Y., Brame, C.J., Shabanowitz, J., Hunt, D.F., and Woolford, J.L. Jr. (2001) Composition and functional characterization of yeast 66S ribosome assembly intermediates. *Mol. Cell* **8**, 505–515
10. Oeffinger, M., Leung, A., Lamond, A., and Tollervey, D. (2002) Yeast Pescadillo is required for multiple activities during 60S ribosomal subunit synthesis. *RNA* **8**, 626–636
11. Liu, Y. and Chang, A. (2009) A mutant plasma membrane protein is stabilized upon loss of Yvh1, a novel ribosome assembly factor. *Genetics* **181**, 907–915
12. Zuk, D., Belk, J.P., and Jacobson, A. (1999) Temperature-sensitive mutations in the *Saccharomyces cerevisiae MRT4*, *GRC5*, *SLA2* and *THS1* genes result in defects in mRNA turnover. *Genetics* **153**, 35–47
13. Lo, K.Y., Li, Z., Wang, F., Marcotte, E.M., and Johnson, A.W. (2009) Ribosome stalk assembly requires the dual-specificity phosphatase Yvh1 for the exchange of Mrt4 with Rpp0. *J. Cell Biol.* **186**, 849–862
14. Kemmler, S., Occhipinti, L., Veisu, M., and Panse, V.G. (2009) Yvh1 is required for a late maturation step in the 60S biogenesis pathway. *J. Cell Biol.* **186**, 863–880
15. Wilson, W.A., Wang, Z., and Roach, P.J. (2002) Systematic identification of the genes affecting glycogen storage in the yeast *Saccharomyces cerevisiae*: implication of the vacuole as a determinant of glycogen level. *Mol. Cell. Proteomics* **1**, 232–242
16. Cannon, J.F., Pringle, J.R., Fiechter, A., and Khalil, M. (1994) Characterization of glycogen-deficient glc mutants of *Saccharomyces cerevisiae*. *Genetics* **136**, 485–503
17. Enyenihi, A.H. and Saunders, W.S. (2003) Large-scale functional genomic analysis of sporulation and meiosis in *Saccharomyces cerevisiae*. *Genetics* **163**, 47–54
18. Anderson, J.S. and Parker, R.P. (1998) The 3′ to 5′ degradation of yeast mRNAs is a general mechanism for mRNA turnover that requires the SKI2 DEVH box protein and 3′ to 5′ exonucleases of the exosome complex. *EMBO J.* **17**, 1497–1506
19. van Hoof, A., Lennertz, P., and Parker, R. (2000) Yeast exosome mutants accumulate 3′-extended polyadenylated forms of U4 small nuclear RNA and small nucleolar RNAs. *Mol. Cell. Biol.* **20**, 441–452
20. Thomas, B.J. and Rothstein, R. (1989) Elevated recombination rates in transcriptionally active DNA. *Cell* **56**, 619–630
21. Amberg, D.C., Burke, D.J., and Strathern, J.N. (2005) *Methods in yeast genetics*., Cold Spring Harbor Laboratory Press, Cold Spring Harbor, NY
22. Roberts, T.M., Swanberg, S.L., Poteete, A., Riedel, G., and Backman, K. (1980) A plasmid cloning vehicle allowing a positive selection for inserted fragments. *Gene* **12**, 123–127
23. Sikorski, R.S. and Hieter, P. (1989) A system of shuttle vectors and yeast host strains designed for efficient manipulation of DNA in *Saccharomyces cerevisiae*. *Genetics* **122**, 19–27
24. Wang, Z., Wilson, W.A., Fujino, M.A., and Roach, P.J. (2001) Antagonistic controls of autophagy and glycogen accumulation by Snf1p, the yeast homolog of AMP-activated protein kinase, and the cyclin-dependent kinase Pho85p. *Mol. Cell. Biol.* **21**, 5742–5752

25. Parker, R., Herrick, D., Peltz, S.W., and Jacobson, A. (1991) Measurement of mRNA decay rates in *Saccharomyces cerevisiae*. *Methods Enzymol*. **194**, 415–423
26. Hermansyah., Sugiyama, M., Kaneko, Y., and Harashima, S. (2009) Yeast protein phosphatases Ptp2p and Msg5p are involved in G1-S transition, *CLN2* transcription, and vacuole morphogenesis. *Arch. Microbiol.* **191**, 721–733
27. Muda, M., Manning, E.R., Orth, K., and Dixon, J.E. (1999) Identification of the human YVH1 protein-tyrosine phosphatase orthologue reveals a novel zinc binding domain essential for in vivo function. *J. Biol. Chem*. **274**, 23991–23995
28. Remacha, M., Jimenez-Diaz, A., Santos, C., Briones, E., Zambrano, R., Rodriguez Gabriel, M.A., Guarinos, E., and Ballesta, J.P. (1995) Proteins P1, P2 and P0, components of the eukaryotic ribosome stalk. New structural and functional aspects. *Biochem. Cell Biol*. **73**, 959–968
29. Santos, C. and Ballesta, J.P.G. (2005) Characterization of the 26S rRNA-binding domain in *Saccharomyces cerevisiae* ribosomal stalk phosphoprotein Rpp0. *Mol. Microbiol*. **58**, 217–226
30. Venema, J. and Tollervey, D. (1999) Ribosome synthesis in *Saccharomyces cerevisiae*. *Annu. Rev. Genet*. **33**, 261–311
31. Herrick, D., Parker, R., and Jacobson, A. (1990) Identification and comparison of stable and unstable mRNAs in *Saccharomyces cerevisiae*. *Mol. Cell. Biol*. **10**, 2268–2284
32. Rodríguez-Mateos, M., Abia, D., García-Gómez, J.J., Morreale, A., de la Cruz, J., Santos, C., Remacha, M., and Ballesta, J.P. (2009) The amino terminal domain from Mrt4 protein can functionally replace the RNA binding domain of the ribosomal P0 protein. *Nucleic Acids Res*. **37**, 3514–3521
33. Kresse, S.H., Berner, J.M., Meza-Zepeda, L.A., Gregory, S.G., Kuo, W.L., Gray, J.W., Forus, A., and Myklebost, O. (2005) Mapping and characterization of the amplicon near *APOA2* in 1q23 in human sarcomas by FISH and array CGH. *Mol. Cancer* **4**, 39
34. Montanaro, L., Treré, D., and Derenzini, M. (2008) Nucleolus, ribosomes, and cancer. *Am. J. Pathol*. **173**, 301–310